SIMULATION OF INTERNAL WAVE WAKES AND COMPARISON WITH OBSERVATIONS

James K.E. Tunaley

London Research and Development Corporation,
114 Margaret Anne Drive, Ottawa, K0A 1L0, Canada.
Email:JTunaley@London-Research-and-Development.com

ABSTRACT

The Loch Linnhe trials took place from 1989 to 1994 in Scotland and were designed to evaluate the use of ship-generated internal waves for maritime surveillance by high resolution radar. The crest structure of the observed wakes is understood but the conditions under which an internal wave wake can be observed by high resolution radar are still obscure. The purpose of this paper is to describe simulated wakes using a simple model and to compare the results with the observations; this relies on estimating and comparing the surface flow velocities that affect the Bragg waves and the resultant radar backscatter. The surface flow velocities produced by two practical hull forms (Taylor, Series 60) as well as the Wigley form are calculated. It turns out that simple models can explain the broad characteristics of internal wave wake generation by surface ships moving near the vertical density profile appropriate to a narrow horizontally stratified internal layer.

1. INTRODUCTION

1.1. Objectives

Ship-generated internal wave wakes have been observed in both airborne [1] and space-borne Synthetic Aperture Radar (SAR) such as in the ERS1 image of the Georgia Strait in Fig. 1. Though seemingly quite rare, they could be important for wide-area maritime surveillance by high resolution space based microwave radar. However, the generation of these wakes is not fully understood. For example, the crest patterns can be calculated with reasonable accuracy but there are neither reported satisfactory predictions of the amplitudes of the individual waves within the wake nor comparisons with observation, at least in the unclassified literature. A proper understanding would enable the conditions under which internal wave wakes are generated to be determined and the utility of internal wave wakes for ocean surveillance to be assessed.

The radar returns are related to the hydrodynamic fluctuations on the surface and in particular those that are associated with the wake. Because vertical surface displacements associated with internal waves are usually very small [2], the principal imaging mechanism appears to involve fluctuations in the surface velocity of the water [1]. This affects the distribution of Bragg waves that are mainly responsible for the radar backscatter. The present study focuses on the surface velocities induced by a wake. According to Hogan [1], surface velocities of the order of 1 cm/s (and probably much less) are sufficient to create observable wakes in radar imagery in the Ku and Ka microwave radar bands.

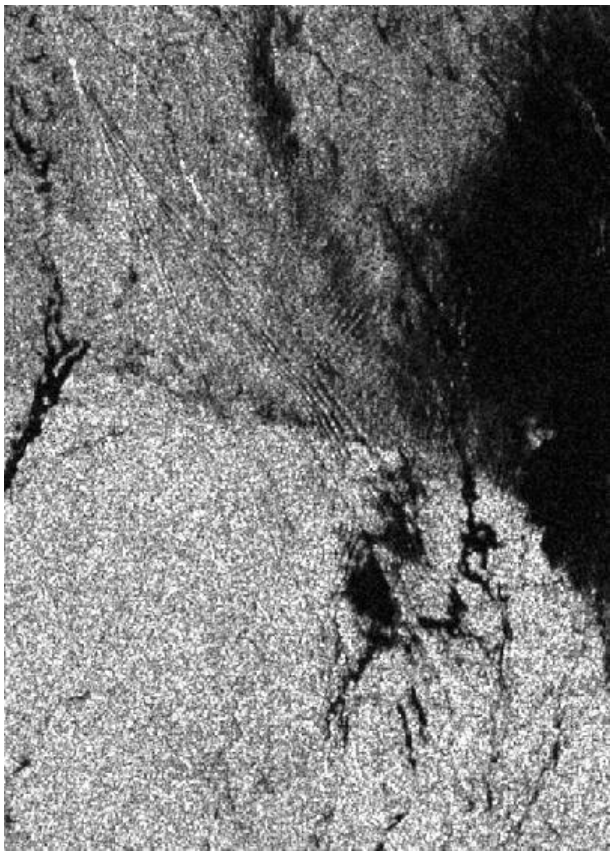

Figure 1. ERS1 Image of internal wave wakes.

This report describes simulations of the internal wave wakes from ships and compares them with those observed during the Loch Linnhe trials. These trials were part of a US/UK initiative. They were designed to investigate the occurrence of observable internal wave wakes in radar. Because internal waves can propagate horizontally on the interface between fresh and salt water, a loch can be an ideal location. However, the

propagation of internal waves is generally complicated because, in the open ocean for example, the density changes are not usually as abrupt as can occur in a loch.

1.2. Modelling

A horizontal internal layer is characterized principally by its vertical density profile. It can be modelled simplistically as a simple abrupt jump in the water density as a function of depth or more realistically as a slow change in density. The first model represents a "discrete" internal layer and the second a "diffuse" layer. In a loch, the first model may be a sufficiently good approximation. This can be understood by noting that, though many modes of oscillation in a diffuse layer are possible, only the lowest sinuous mode and occasionally the next (varicose) mode are likely to be relevant for ship wakes. This is because only the lowest mode is likely to be excited efficiently as a moving ship pushes the water downwards to create a wave on the layer and because the propagation velocities of the lowest mode are greatest and give the widest wake contributions.

In both layer models, the theory, which has been described in [3] and [4], employs a linear approximation, which should be appropriate except near to the ship. This should not represent a great problem as radar wakes are primarily far field phenomena. However, the amplitudes of the wake waves will be affected by this approximation and very close agreement between theory and observation is certainly not guaranteed. For general maritime surveillance this is not important because the characteristics of the ship will often not be known to the detail required to simulate an accurate wake. In principle accurate wakes might be simulated using Computation Fluid Dynamics (CFD). For example, Chang et al. [5] have simulated internal wave wakes of submarines. This uses the simplified discrete layer model but it is not likely that their approach could be operationally effective in the foreseeable future. This is because of the excessive time taken to run simulations of this type.

It is assumed that wake production from the ship hull can be modelled by a distribution of sources and sinks of fluid moving horizontally at constant velocity; a sink is just a negative source. There are several common methods of representing the hull of a ship. The hull can be represented by a distribution of dipole sources and sinks on the hull itself [6]. The strength of each dipole can be chosen so that fluid velocity on the hull matches the actual velocity. A simpler approach, which is used here, is to place sources and sinks on the ship's longitudinal vertical centre plane [4]; again the idea is to ensure that the simulated fluid flow near the hull matches the actual velocities. This is called the "thin ship model". The former method can be implemented accurately, at least in principle. In the latter method, the fluid vector velocities near the hull can only be matched approximately. Additional complications arise from the presence of a turbulent boundary layer, the pressure changes due to the propulsion system and a collapsing turbulent wake [7]; these will be addressed later.

It can be shown that the crest patterns of a far-field internal wave wake are only a function of the ship speed and the phase and group velocities of the internal waves [1], [8]. The crest shapes are not affected by the distribution of the sources or their depth. However, the amplitudes do depend on the source distribution and the depths of the sources are important.

Also the waves created by a source at one position will interfere with those from another source displaced from it. Therefore the shape and dimensions of the hull influence the wave amplitudes.

In the present context, those wakes that are stationary in the reference frame of the ship fall into two categories. In the first category the ship speed is less than the maximum speed of the internal waves. The wake resembles the Kelvin wake with transverse and divergent wave systems. The second category represents the super-critical case where the ship is moving faster than the maximum speed of the wake waves. Wakes in the second category comprise only divergent waves. This can be understood by noting that exactly transverse waves cannot propagate at the ship speed (by definition). Because the maximum speed of internal waves is usually much less than 1 m/s, only the super-critical case is treated here.

1.3. Loch Linnhe Trials

In the Loch Linnhe trials, ship displacements ranged from 100 tons to nearly 30,000 tonnes and data were acquired for various wind speeds up to 15 m/s. Compared with the open ocean, the peak Brunt-Väisälä (B-V) frequencies were quite high ranging from 0.02 rad/s to 0.17 rad/s. The associated depths ranged from 1 m to 17 m. An example of a B-V profile, taken from Watson et al. [8] is shown in Fig. 2. Here N denotes the B-V frequency. In this profile the layer is concentrated between depths of about 1 m and 6 m, say.

Tab. 1 shows a list of the principal ships used in the trials, derived from [8]. The ship speeds typically ranged from 1 m/s to 4 m/s and occasionally up to 6 m/s. The beam used in the simulations is the maximum ship width at the waterline. For the Sir Tristram, this is probably about 17 m (from the Internet). Also the length of this ship at the waterline was probably 136 m. This is because it was badly damaged in the Falklands war and was rebuilt and lengthened in 1985. These dimensions differ from those quoted in [8], which appear to

represent the ship before 1982. The Sir Tristram was decommissioned in 2005.

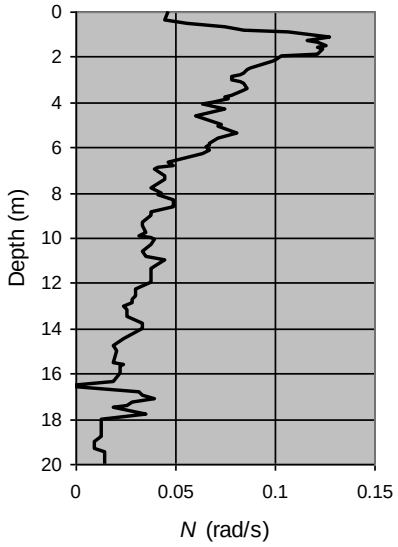

Figure 2. Example of a Loch Linnhe B-V frequency profile, from [8].

The imaging radars were airborne and ranged in frequency from P-band to Ku band.

2. HULL DESIGNS

In this report the models are distinguished by their block coefficient, C_B (as recommended in [10]). This represents the ratio of the volume of the hull under water to the volume of a rectangular parallelepiped into which the submerged part of the hull just fits.

Hulls designed for warships typically exhibit block coefficients of the order of 0.5, while C_B for cargo ships often lies in a range 0.70 to 0.85.

The Wigley hull form is often used in simulations because it can be represented by simple parabolic functions [9]. It can be used as a baseline hull to evaluate the effects introduced by other practical hulls. The Wigley hull resembles the hull of a canoe and its block coefficient can range from 0.36 to 0.53 Only the very simplest Wigley form, known as the "parabolic form" is used here and its block coefficient is 0.44. A version of the Wigley offsets is shown in Fig. 3. This shows the shape of the transverse hull sections at stations (not necessarily evenly spaced) along the longitudinal axis of the ship; the horizontal line represents the waterline and the hull above it is freeboard.

The practical shape of a ship's hull is usually subject to various constraints. A principal constraint is the requirement to minimize the resistance to forward motion. Other constraints involve sea-keeping, operating speed, and cargo capacity. Hull optimization for a normal single-hulled cargo or warship usually results in a hull form that can be derived from some basic streamlined shape. There exists a variety of these; examples are shown in Tab. 2. In this report the hull shapes are based on the Taylor methodical series, which is appropriate to twin-screwed warships and has been re-analyzed [11] and on the Series 60 series developed by the David Taylor Model Basin (DTMB) [12]. The latter is appropriate to single screwed cargo ships.

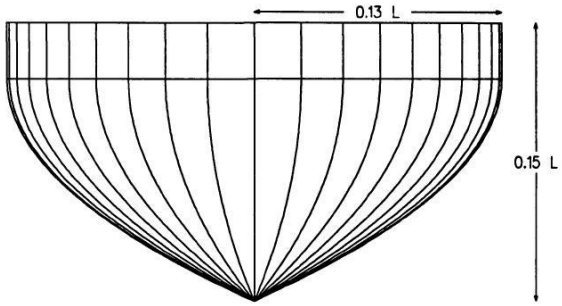

Figure 3. Wigley hull offsets, from [9].

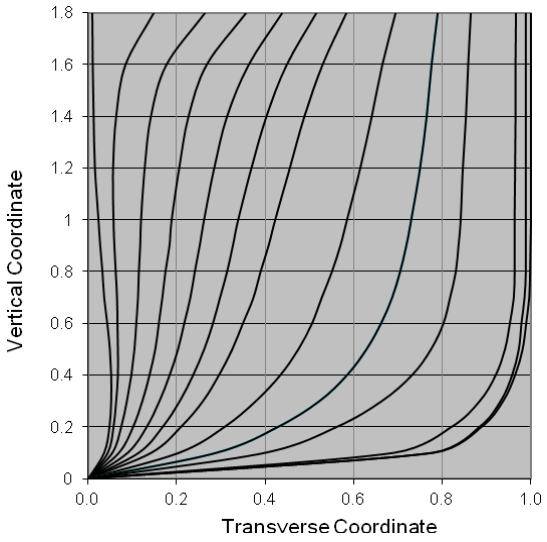

Figure 4. Taylor parent bow offsets (from [13]).

Table 1. Trials ships according to Watson et al [8].

Name	Type	Length (m)	Beam (m)	Draft (m)	Displacement (tonnes)
Roysterer	Ocean Tug	51	12	5.5	1400
Sir Tristram	Heavy Landing Ship	116	20	3.9	5300
Blue Rover	Small Fleet Tanker	141	19	7	12000
Olmeda	Fleet Oiler	180	26	9.2	29000

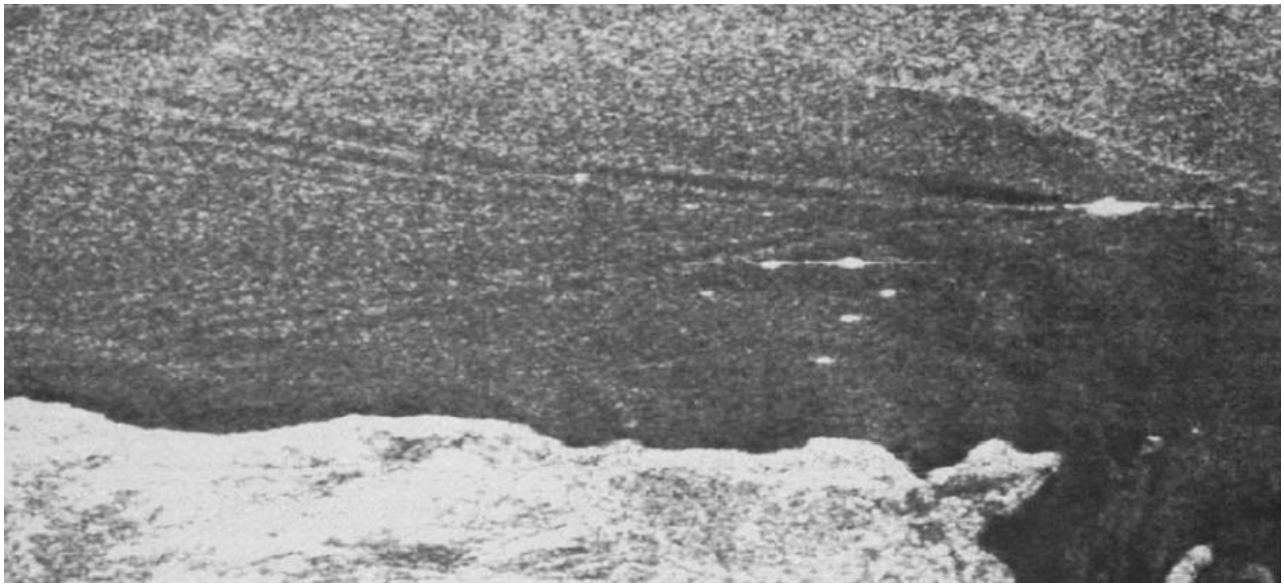

Figure 5. Radar image of the Sir Tristram wake. Ship speed is 2.0 m/s (from [8]). The bright spots to the right of the centre are the locations of sensor buoys.

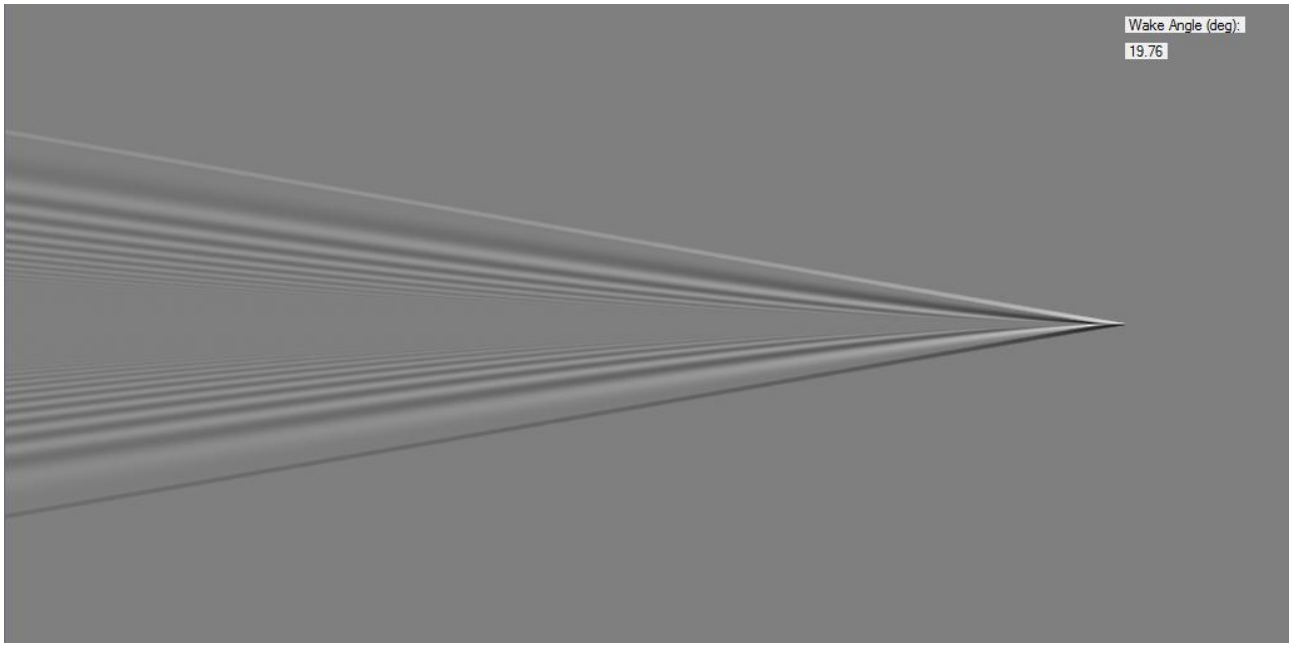

Figure 6. Cross-track velocity simulation of Sir Tristram wake using the Wigley hull; layer depth, h = 5m.

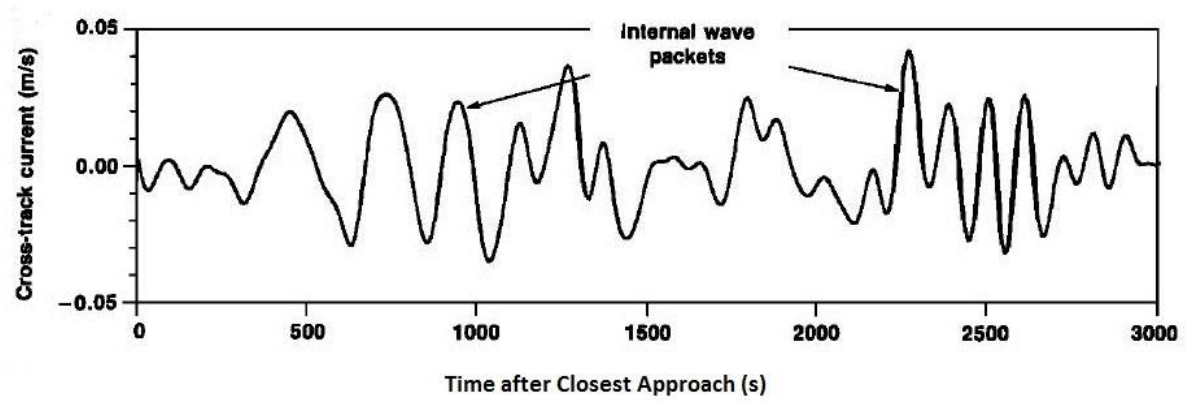

Figure 7. Cross-track current as a function of time.

Table 2. Standard hull form examples

Hull Form	**Remarks**
Taylor Standard Methodical Series	Round-bilge. Displacement hulls. Often used for twin screw warships.
David Taylor Model Basin (DTMB) Series 60	Round bilge, single screw merchant ship.
National Physical Laboratory (NPL) Series	Round-bilge. High speed displacement hulls.
National Technical University of Athens (NTUA) Series	Double chine. Planing hull form.
United States Coast Guard (USCG) Series	Double chine with second chine just below deck. High speed planing hulls.
British Ship Research Association (BSRA) Series	Round-bilge. High block coefficient. Used for cargo ships.
US Maritime Administration (MARAD) Series	Round-bilge, single screw merchant ship, low speed. High block coefficient with high beam to draft ratio. Used for cargo ships in shallow waters.

The original Taylor series was based on the British cruiser "Leviathan"; the parent hull form is based on a modified version. In [11], a digital algorithm for developing the series members is described, which employs polynomial approximations of order 5 in the longitudinal distance. This mimics the graphical method used formerly. Details of the method, some corrections and a change in the principal parameter from prismatic coefficient to block coefficient are provided in [13].

The bow section hull offsets for the normalized parent model are shown in Fig. 4. The vertical coordinate is the normalized distance from the keel; 1.0 represents the nominal waterline. The horizontal coordinate is the normalized horizontal distance from the longitudinal vertical centreplane. As can be seen, the Taylor form includes a bulb at the bow.

Offspring are derived from the parent by shifting the offsets longitudinally in a prescribed manner based on the prismatic coefficient. Because the shape of the hull at mid-ships does not change during this procedure and its area coefficient is given, it is possible to relate the block coefficient directly to the prismatic coefficient using a constant factor [13].

The DTMB Series 60 models are tabulated in [12] for block coefficients from 0.6 to 0.8 at intervals of 0.05. This form does not exhibit a bulbous bow. There are other significant differences from the Taylor model at the stern because only one screw is needed rather than two.

3. SIMULATIONS

The simulations were conducted using the discrete layer model. This reduces the number of variables required to describe the internal layer; the variables are the layer depth, which is the depth (h) of the interface at which there is an abrupt change in density, and the layer strength (δ), which is the fractional increase in density as the interface is traversed in a downwards direction. The angle of the internal wave wake, β, is given by:

$$\sin(\beta/2) = \sqrt{g\delta h}/U\,, \qquad (1)$$

where g is the acceleration due to gravity and U is the ship speed. For a given wake angle, the layer parameters are constrained by Eq. 1.

Fig. 5 shows a radar image of the wake of the Sir Tristram from [8]. This was taken with airborne L-band (1.26 GHz) synthetic aperture radar with VV polarization; the incidence angle was 40º. The pixel size was about 4 m by 4 m and the length of the image is about 4.1 km. The ship speed is 2 m/s, the wake angle is

about 20º and appropriate layer parameters (h, δ) could be for example (5.0 m, 0.0024) or (3.0 m, 0.004).

While the Wigley hull together with its derivatives, which are required for the source distribution, can be described analytically, the Taylor and DTMB hulls are generally provided as tables of offsets. These practical data are sparse and there is an assumption of smoothness. Therefore cubic splines are fitted to the offsets in both the longitudinal and vertical directions to obtain offsets and derivatives at the required locations.

Fig. 6 shows the simulated cross-track component of the surface velocity wake corresponding to the observed wake in Fig. 5. This is for the Wigley hull. The layer depth is set at 5 m, the ship length, beam, draft and speed are 136 m, 17 m, 4 m and 2 m/s respectively. When taking into account the noise in the radar image, the crest patterns of the observed and simulated wakes are reasonably similar.

The cross-track currents at various depths were observed as the ship passed set of sensors located about 169 m from the ship's track. From the sensor data, the horizontal cross-track velocity component at the surface was estimated [8]. This is shown in Fig. 7. To reduce the effect of ambient noise, the original signals were band-pass filtered. This filtering also removed some of the structure in the data. Also, it is likely that the effects from wave reflections at the shore line are visible in the later part of the record. The corresponding simulated current using a Wigley hull is shown in Fig. 8.

As expected, both the observed and simulated records indicate that the wake reaches a sensor at about 500 s after the passage of the ship. There are about 6 oscillations between 500 s and 1500 s in both records. There is a suggestion of a shoulder during the first major oscillation in the observed record but this is very prominent in the simulated record. However, the amplitude in the simulated record is too small being less than one half of the observed value.

When the layer in the simulation is raised to a depth of 3 m, the result is shown in Fig. 9. Now the amplitudes of the observed and simulated records are similar as is the general shape of the first 3 oscillations but there are too many oscillations in the simulation.

Additional plots of the simulated velocities that are analogous to Fig. 6 are not shown. This is because it is difficult to distinguish them from Fig. 6.

The shoulder arises because waves from the bow section arrive at a sensor before those from the stern section of the ship. Sources generally represent the bow while sinks represent the stern. Sinks tend to cancel sources depending on the phases of the waves that they generate. The effect can be seen in Fig. 10, which shows the bow and stern contributions separately as well as their sum, which is the same as in Fig. 8.

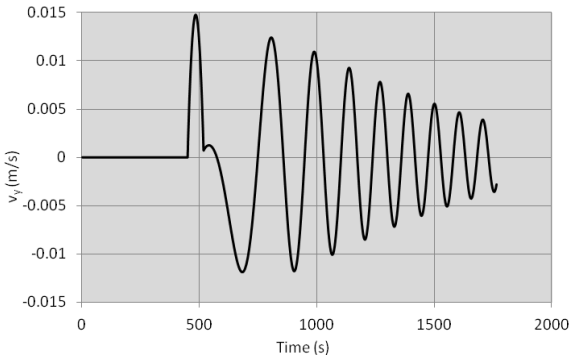

Figure 8. Simulated cross-track surface velocity component using Wigley hull and h = 5m.

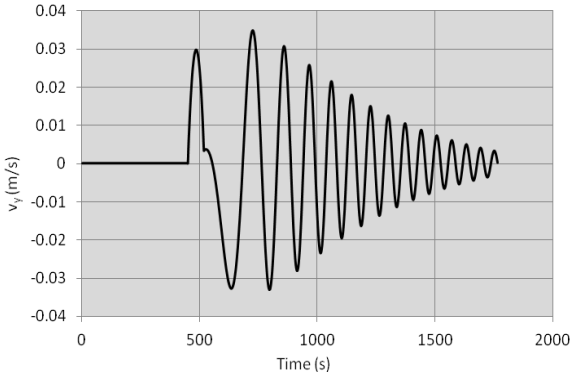

Figure 9. Simulated cross-track surface velocity component using Wigley hull and h = 3m.

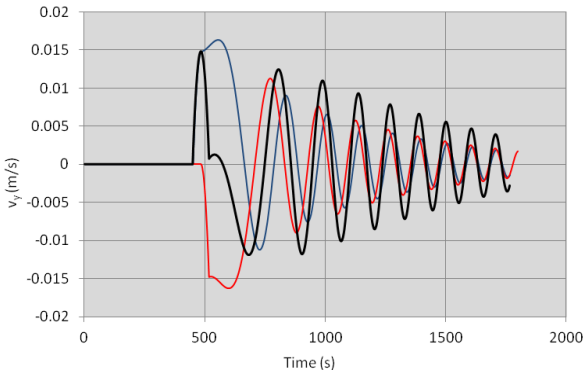

Figure 10. Bow and stern velocity profiles; bow (—), stern (—), total (—). Layer depth h = 5 m.

Figs. 11 and 12 show the cross-track surface velocity component for the Taylor models using block coefficients of 0.48 and 0.7 respectively; the layer depth is 5 m. These plots closely resemble the corresponding plot for the Wigley hull for which the block coefficient

is 0.44, though there are some differences. The main difference is the shoulder, which is located at a different cross-track velocity.

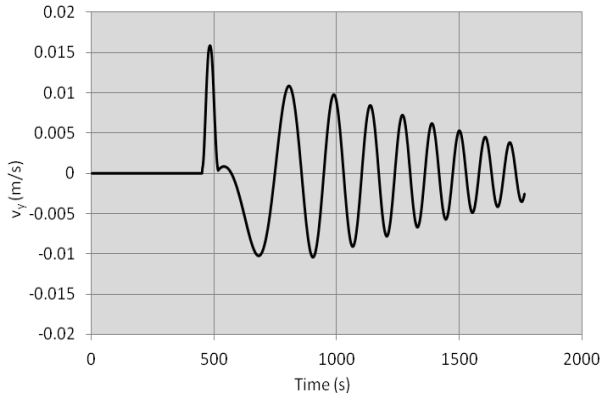

Figure 11. Taylor model C_B = 0.48; h = 5 m.

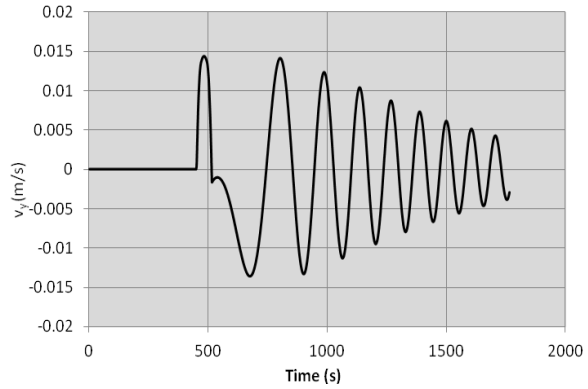

Figure 12. Taylor model C_B = 0.70; h = 5 m.

Similarly, Figs. 13 and 14 show the cross-track surface velocity component for the DTMB models using block coefficients of 0.6 and 0.8 respectively. Once again the results for the smaller block coefficient resemble those of the Wigley hull. On the other hand the shoulder is now moved to a distinctly new position in the plot. This is associated with the fact that the sources and sinks are concentrated near the bow and stern when the block coefficient is large.

It is noted that the qualitative characteristics of the plots remain the same if the depth of the layer is changed to 3 m; the maximum amplitudes are increased from about 0.01 m/s to about 0.03 m/s and the number of oscillations is increased as with the Wigley hull.

Stapleton [14] has presented some data for the Olmeda. The block coefficient can be estimated from Tab. 1 as 0.67. According to [14], the internal wave wake angle was about 18º and, assuming that the layer parameters were (3 m, 0.004), the ship speed must have been about 2.2 m/s. Using the Taylor hull model, the simulated cross-track velocity at the sensor located 169 m from the ship track is shown in Fig. 15. The maximum absolute amplitude is now a little greater than 5 cm/s.

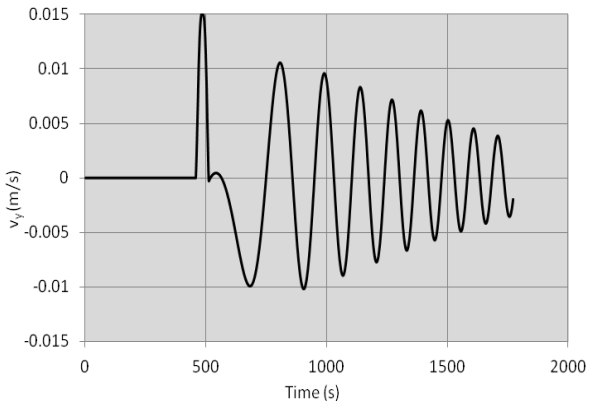

Figure 13. DTMB model C_B = 0.6; h = 5m.

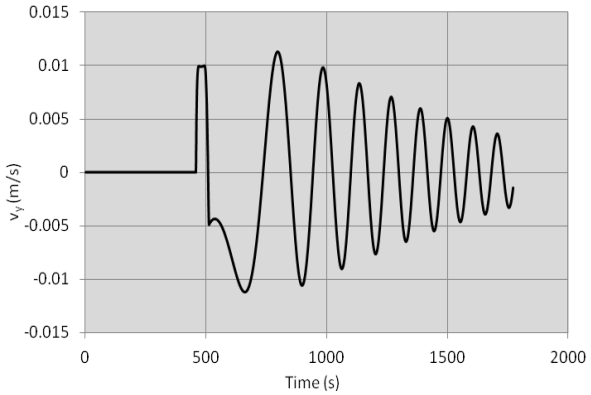

Figure 14. DTMB model C_B = 0.8; h = 5 m.

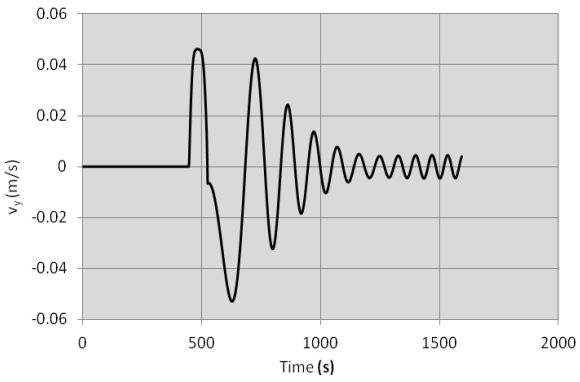

Figure 15. Olmeda cross-track velocity.

This is consistent with remarks made in both [8] and [14].

4. DISCUSSION

Considering the ambient noise on all the observations, the band-pass filtering on the estimation of the surface velocities and the uncertainties regarding the hull, there

is satisfactory agreement between the simulations and the available observations of the wake crest pattern derived from the radar. There is also satisfactory agreement between the estimated and the simulated surface velocities. However, good agreement cannot be achieved without changing the simulated depth of the discrete layer, though it is always in an acceptable range. These results are almost independent of the hull model. The simulations could probably be improved considerably by using the diffuse layer model.

As noted earlier, the presence of a turbulent wake, the effects of a collapsing wake (due to mixing within the turbulent wake) and pressure changes due to the propulsion system can affect the wake production near the stern. In principle these could also account for the discrepancies but this is unlikely because the velocity profiles do not seem to be very sensitive to the stern shape.

Using the discrete internal layer, it appears that there is little difference in the simulated internal wave wake amplitudes as a function of hull model except when the block coefficient is quite high as is often the case for merchant vessels. The difference is primarily in the position of the shoulder in the velocity plot. In a radar image of an internal wave wake this corresponds to positions just inside the wake edge. Reference to Fig. 5, suggests that it might be difficult to observe the shoulder in a radar image without some significant additional processing and optimization of the radar.

4.1. Wake Detection

An operational system designed to detect internal wave wakes from radar imagery will be subject to a detection requirement; this will involve probabilities of detection and false alarm as well as conditions that must be satisfied. For example, internal wave wakes can only be observed if there is an internal layer present that itself meets certain conditions. Moreover the wind and principal wave vectors must be within limits. Therefore a wake detection software application must involve additional information some of which may be statistical or be derived terrestrially.

5. REFERENCES

1. Hogan, G.G. (1991). Correlation of Ku-band and Ka-band SAR Imaged Internal Wave Modulations with In-Water Current Measurements, *IEEE Proc. Oceans '91*, Ocean Technologies and Opportunities in the Pacific for the '90s, pp 818-825.

2. Phillips, O.M. (1980). *The Dynamics of the Upper Ocean*, 2nd Ed., Cambridge University Press, London.

3. Tunaley, J.K.E. (2012). The Theory of Internal Wave Wakes, DRDC Ottawa Contractor Report, CR 2012-119, March.

4. Tunaley, J.K.E. (2013). Simulations of Internal Wave Wakes from the Loch Linnhe Trials, DRDC Ottawa Contractor Report, CR 2013-048, January.

5. Chang, Y., Zhao, F., Hong, F-W, Li, P. and Yun, J. (2006). Numerical Simulation of Internal Waves Excited by a Submarine in a Two-Layer Stratified Fluid, *J. Hydrodynamics*, Series B, Vol. 18, No. 3 Supplement, pp 330-336.

6. Vernon, T.A., Bara, B. and Hally, D. (1988), "A surface panel method for the calculation of added mass matrices for finite element models", DRDC Atlantic Technical Memorandum 88/203, February.

7. Schooley, A. and Stewart, R.W. (1963). Experiments with a Self-Propelled Body Submerged in a Fluid with a Vertical Density Gradient, *J. Fluid Mech.*, Vol 15(1), pp 83-96.

8. Watson, G., Chapman, R. and Apel, J. (1992). Measurements of the Internal Wave Wake of a Ship in a Highly Stratified Sea Loch, *J. Geophys. Res.*, Vol. 97, No. C6, pp 9689-9703, June.

9. Hally, D. (1989). Representation of Wigley Hulls by HLLSRF, Defence Research Establishment Atlantic, Technical Communication 89/308, September.

10. Molland, A., Turnock, S.R. and Hudson, D.A. (2011). *Ship Resistance and Propulsion: Practical Estimation of Ship Propulsive Power*, Cambridge University Press, New York.

11. Gertler, M. (1954). *A Reanalysis of the Original Test Data for the Taylor Standard Series*, David W. Taylor Model Basin Report 806, Washington D.C., March.

12. Todd, F.H. (1963). Series 60 – Methodical Experiments with Models of Single Screw Merchant Ships, David Taylor Model Basin Report 1712, July.

13. Tunaley, J.K.E. (2013). An Examination of the Taylor Standard Series of Hull Forms, LRDC Report, July, http://london-research-and-development.com.

14. Stapleton N.R. (1997). Ship Wakes in Radar Imagery, *Int. J. Remote Sensing*, Vol. 18, No. 6, pp 1381-1386.